Inorg. Chem. **2005**, *44*, 996–1005

Anion-Dependent Silver(I) Coordination Polymers of the Tridentate Pyridylphosphonite: $PPh(3\text{-}OCH_2C_5H_4N)_2$

Rodney P. Feazell, Cody E. Carson, and Kevin K. Klausmeyer*

Department of Chemistry and Biochemistry, Baylor University, Waco, Texas 76798

Received September 28, 2004

Three new multidimensional coordination polymers have been constructed from the reaction of AgX, where X = OTf^-, BF_4^-, or tfa^-, with the novel phosphonite $PhP(3\text{-}OCH_2C_5H_4N)_2$, **PCP-32**, **1**. It is seen that regardless of the ratio of reactants mixed, polymeric growth of the compounds always reveals a ligand-to-metal ratio of 1:2 for **PCP-32AgOTf**, **2**, 1:1 for **PCP-32AgBF$_4$**, **3**, and 1:2 for **PCP-32Ag(tfa)**, **4**. The coordination number, metal environment, ligand conformation, and polymer dimensionality are found to vary greatly from **2** to **4** and are dependent upon the anion present. Coordination numbers from 2 to 4, representing linear, trigonal, and distorted tetrahedral environments are displayed. **PCP-32AgOTf** polymerizes as a linear chain containing both two- and four-coordinate silvers, **PCP-32AgBF$_4$** repeats a single trigonal motif throughout its structure, and **PCP-32Ag(tfa)** shows two unique distorted tetrahedral silver centers. Ligand flexibility allows for cross-ligand Ag–Ag distances to range from 3.1918(8) to 14.015(2) Å. The coordination polymers have been characterized by elemental analysis, variable-temperature multinuclear NMR spectroscopy, single-crystal X-ray diffraction, and fluorometric studies.

Introduction

The self-assembly of coordination polymers that offer a variety of novel structural, electronic, optical, catalytic, and medicinal properties is currently an intense area of study in supramolecular chemistry.[1−6] Specific attention has been given to those structures based upon the coinage metals.[1,3,7,8] In particular, coordination polymers involving the silver(I) ion have made a large contribution to this field due in part to the ease with which it varies its coordination number.[9−29] The fact that silver(I) can readily vary its coordination number from 2 to 6 by merely changing the size or concentration in solution of a ligating species makes it an appealing candidate for use in deliberately designed or

* To whom correspondence should be addressed. E-mail: Kevin_Klausmeyer@baylor.edu.

(1) Zheng, S.-L.; Tong, M.-L.; Chen, X.-M. *Coord. Chem. Rev.* **2003**, *246*, 185−202.
(2) Erxleben, A. *Coord. Chem. Rev.* **2003**, *246*, 203−228.
(3) Lu, J. Y. *Coord. Chem. Rev.* **2003**, *246*, 327−347.
(4) Khlobystov, A. N.; Blake, A. J.; Champness, N. R.; Lemenovskii, D. A.; Majouga, A. G.; Zyk, N. V.; Schröder, M. *Coord. Chem. Rev.* **2001**, *222*, 155−192.
(5) Blake, A. J.; Champness, N. R.; Hubberstey, P.; Li, W.-S.; Withersby, M. A.; Schroder, M. *Coord. Chem. Rev.* **1999**, *183*, 117−138.
(6) Janiak, C. *J. Chem. Soc., Dalton Trans.* **2003**, *14*, 2781−2804.
(7) Vetrichelvan, M.; Lai, Y.-H.; Mok, K. F. *Eur. J. Inorg. Chem.* **2004**, 2086−2095.
(8) Fournier, E.; Lebrun, F.; Drouin, M.; Decken, A.; Harvey, P. D. *Inorg. Chem.* **2004**, *43*, 3127−3135.
(9) Yang, J.-H.; Zheng, S.-L.; Yu, X.-L.; Chen, X.-M. *Cryst. Growth Design* **2004**, *4*, 831−836.
(10) Fan, J.; Sun, W.-Y.; Okamura, T.-A.; Tang, W.-X.; Ueyama, N. *Inorg. Chem. Acta* **2004**, *357*, 2385−2389.
(11) Bacchi, A.; Bosetti, E.; Carcelli, M.; Pelagatti, P.; Rogolino, D. *Eur. J. Inorg. Chem.* **2004**, 1985−1991.
(12) Sun, D.; Cao, R.; Bi, W.; Li, X.; Wang, Y.; Hong, M. *Eur. J. Inorg. Chem.* **2004**, 2086−2095.
(13) Adachi, K.; Kaizaki, S.; Yamada, K.; Kitagawa, S.; Kawata, S. *Chem. Lett.* **2004**, *33*, 648−649.
(14) Dong, Y.-B.; Wang, P.; Huang, R.-Q.; Smith, M. D. *Inorg. Chem.* **2004**, *43*, 4727−4739.
(15) Kyono, A.; Kimata, M.; Hatta, T. *Inorg. Chem. Acta* **2004**, *357*, 2519−2524.
(16) Aslanidis, P.; Cox, P. J.; Divanidis, S.; Karagiannidis, P. *Inorg. Chem. Acta* **2004**, *357*, 2677−2686.
(17) Liu, H.-M.; Zhang, W.; Zheng, Y.; Zhang, W.-Q. *J. Mol. Struct.* **2004**, *698*, 37−40.
(18) Pickering, A. L.; Cooper, G. J. T.; Long, D.-L.; Cronin, L. *Polyhedron* **2004**, *23*, 2075−2079.
(19) Zou, Y.; Liu, W.-L.; Lu, C.-S.; Wen, L.-L.; Meng, Q.-J. *Inorg. Chem. Commun.* **2004**, *7*, 985−987.
(20) Zhu, H.-F.; Kong, L.-Y.; Okamura, T.-a.; Fan, J.; Sun, W.-Y.; Ueyama, N. *Eur. J. Inorg. Chem.* **2004**, 1465−1473.
(21) Yang, L.; Shan, X.; Chen, Q.; Wang, Z.; Ma, J. S. *Eur. J. Inorg. Chem.* **2004**, 1474−1477.
(22) Westcott, A.; Whitford, N.; Hardie, M. J. *Inorg. Chem.* **2004**, *43*, 3663−3672.
(23) Cheng, J.-K.; Zhang, J.; Kang, Y.; Qin, Y.-Y.; Li, Z.-J.; Yao, Y.-G. *Polyhedron* **2004**, *23*, 2209−2215.
(24) Lu, X. L.; Leong, W. K.; Hor, T. S. A.; Goh, L. Y. *J. Organomet. Chem.* **2004**, *689*, 1746−1756.
(25) Sun, D.; Cao, R.; Bi, W.; Weng, J.; Hong, M.; Liang, Y. *Inorg. Chem. Acta* **2004**, *357*, 991−1001.

10.1021/ic0486365 CCC: $30.25
Published on Web 01/11/2005

"tailored" polymeric coordination complexes.[7,30,31] Other options for controlling structural growth that have proven useful include varying anions to achieve different degrees of interaction or changing the bridging ligand itself to make it more or less rigid.[32,33]

Silver(I) coordination polymers of pyridyl-substituted phosphines are virtually unknown. This could be due to the fact that the majority of work done with pyridyl-substituted phosphines has involved 2-pyridyl substitution.[34−44] The small bite angle associated with the 2-pyridyl substitution inherently limits such a ligand's ability to bridge, and as a result, most complexes of the 2-pyridyl-substituted phosphines are small, discrete structures.[34−41,44] The few reported 3- and 4-pyridyl-substituted phosphines have been sparsely explored in terms of their coordination chemistry and polymer-forming abilities given, at least in part, the difficulty by which these ligands are synthesized and handled.[45−48] We demonstrated recently with the report of the 3-pyridyl-substituted phosphinite, $Ph_2P(3\text{-}OCH_2C_5H_4N)$ or **PCP-31**, that opening the bite angle of these heterobidentate ligands to the point of minimal interaction between the hard and soft binding sites allows the synthesis of some very interesting coordination polymers of various silver(I) salts.[29] The **PCP-nm** naming convention that we have adopted allows for ease in discussion of these pyridylmethylphosphinites as there are many substitutions that can be made and systematic nomenclature can be cumbersome. As such, **PCP** indicates the **p**yridyl**c**arbinol class of **p**hosphorus ligands, where ***n*** is the position of substitution on the pyridyl ring and ***m*** is the number of carbinol substitutions on the phosphorus. As shown in our previous study, the flexibility imparted upon the pyridyl phosphinite ligand by the addition of an $-OCH_2-$ spacer as well as the outwardly oriented binding sites of the meta- and para-nitrogen donors allow for amazing versatility in the coordination modes achievable. A sample of the coordination modes of **PCP-31** that occur with various silver(I) salts is shown in Scheme 1. We have taken our inquiry of the **PCP**s a step further by adding a second pyridyl substitution, effecting a tridentate pyridyl/phosphine donor ligand and expanding the dimensionality available to the coordination polymers formed by ligation to silver(I) salts of various anions. These polymers display a variety of interesting structural and electronic characteristics. The molecular structures and luminescence properties are discussed herein.

Scheme 1. Anion-Dependent Coordination Modes for PCP-31[a]

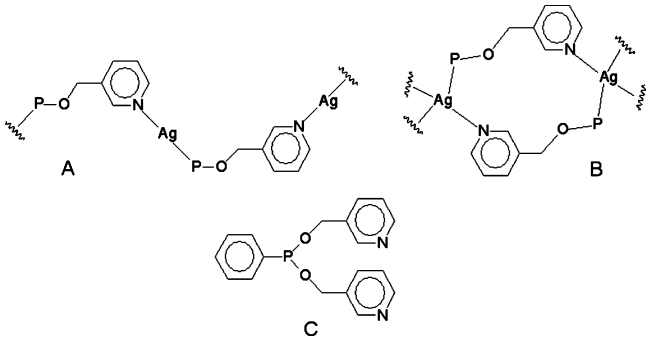

[a] (A) linear chain of ligand-bridged metal centers. (B) Head-to-tail bimetallic cycles anion-bridged into a polymer. (C) Tridentate PCP-32 ligand.

Experimental Section

General Procedures. All experiments were carried out under an argon atmosphere using a Schlenk line and standard Schlenk techniques. Glassware was dried at 120 °C for several hours prior to use. All reagents were stored in an inert atmosphere glovebox; solvents were distilled under nitrogen from the appropriate drying agent immediately before use. Triethylamine was purchased from Aldrich and purged with argon before use. 3-Pyridylcarbinol was purchased from Aldrich and used as received. Dichlorophenylphosphine, silver(I) trifluoroacetate, silver(I) triflate, and silver(I) tetrafluoroborate were purchased from Strem Chemicals Inc. and used as received. Celite was purchased from Aldrich and dried at 120 °C prior to use. ^{1}H and variable-temperature ^{31}P NMR spectra were recorded at 360.13 and 145.78 MHz, respectively, on a Bruker Spectrospin 360 MHz Spectrometer. Elemental analyses were performed by Atlantic Microlabs Inc., Norcross, GA. Excitation and emission spectra were recorded on an Instruments S. A. Inc. model Fluoromax-2 spectrometer using band pathways of 5 nm for both excitation and emission and are presented uncorrected.

Synthesis of Phenylphosphino-bis-3-pyridylcarbinol, $PPh(3\text{-}OCH_2C_5H_4N)_2$, PCP-32 (1). In an argon-purged addition funnel degassed triethylamine (2.28 mL, 16.4 mmol) was added via syringe to a stirred solution of 3-pyridylcarbinol (1.50 g, 13.8 mmol) in 20 mL of toluene at room temperature. The solution was stirred for 15 min, then cooled to 0 °C, and shielded from light with aluminum foil. A solution of dichlorophenylphosphine (1.23 g, 6.87 mmol)

(26) Dong, Y.-B.; Jin, G.-X.; Zhao, X.; Tang, B.; Huang, R.-Q.; Smith, M. D.; Stitzer, K. E.; zur Loye, H.-C. *Organometallics* **2004**, *23*, 1604−1609.
(27) Southward, R. E.; Thompson, D. W. *Chem. Mater.* **2004**, *16*, 1277−1284.
(28) Richards, P. I.; Steiner, A. *Inorg. Chem.* **2004**, *43*, 2810−2817.
(29) Klausmeyer, K. K.; Feazell, R. P.; Reibenspies, J. H. *Inorg. Chem.* **2004**, 1130−1136.
(30) Pickering, A. L.; Long, D.-L.; Cronin, L. *Inorg. Chem.* **2004**, *43*, 4953−4961.
(31) Eisler, D. J.; Puddephatt, R. J. *Cryst. Growth Design* **2004**, in press.
(32) Dong, Y.-B.; Zhao, X.; Huang, R.-Q.; Smith, M. D.; Loye, H.-C. Z. *Inorg. Chem.* **2004**, *43*, 5603−5612.
(33) Seward, C.; Chan, J.; Song, D.; Wang, S. *Inorg. Chem.* **2003**, *42*, 1112−1120.
(34) Song, H.-B.; Zhang, Z.-Z.; Mak, T. C. W. *J. Chem. Soc., Dalton Trans.* **2002**, 1336−1343.
(35) Del Zotto, A.; Zangrando, E. *Inorg. Chem. Acta* **1998**, *277*, 111−117.
(36) Driess, M.; Franke, F.; Merz, K. *Eur. J. Inorg. Chem.* **2001**, *2001*, 2661−2668.
(37) Catalano, V. J.; Kar, H. M.; Bennett, B. L. *Inorg. Chem.* **2000**, 121−127.
(38) Kuang, S.-M.; Zhang, L.-M.; Zhang, Z.-Z.; Wu, B.-M.; Mak, T. C. W. *Inorg. Chem. Acta* **1999**, *284*, 278−283.
(39) Yam, V. W.-W.; Yu, K.-L.; Cheng, C.-C.; Yeung, P. K.-Y.; Cheung, K.-K.; Zhu, N. *Chem. Eur. J.* **2002**, *8*, 4121−4128.
(40) Yam, V. W.-W.; Yeung, P. K.-Y.; Cheung, K.-K. *Angew. Chem., Int. Ed. Engl.* **1996**, *35*, 739−740.
(41) Berners-Price, S. J.; Bowen, R. J.; Harvey, P. J.; Healy, P. C.; Koutsantonis, G. A. *J. Chem. Soc., Dalton Trans.* **1998**, 1743.
(42) Aucott, S. M.; Slawin, A. M. Z.; Woollins, J. D. *Dalton Trans.* **2000**, 2559−2575.
(43) Slagt, V. F.; Reek, J. N. H.; Kamer, P. C. J.; van Leeuwen, P. W. N. M. *Angew. Chem., Int. Ed.* **2001**, *40*, 4271−4274.
(44) Cheshire, P.; Slawin, A. M. Z.; Woollins, J. D. *Inorg. Chem. Commun.* **2002**, *5*, 803−804.
(45) Weisman, A.; Gozin, M.; Kraatz, H.-B.; Milstein, D. *Inorg. Chem.* **1996**, *35*, 1792−1797.
(46) Newkome, G. R. *Chem. Rev.* **1993**, *93*, 2067−2089.
(47) Bowen, R. J.; Garner, A. C.; Berners-Price, S. J.; Jenkins, I. D.; Sue, R. E. *J. Organomet. Chem.* **1998**, *554*, 181−184.
(48) Boggess, R. K.; Zatko, D. A. *J. Coord. Chem* **1973**, *4*, 217−224.

Table 1. Crystallographic Data for 2−4

	2, **PCP-32AgOTf**	**3**, **PCP-32AgBF$_4$**	**4**, **PCP-32Ag(tfa)**
formula	$C_{20}H_{17}Ag_2F_6N_2O_8PS_2 \cdot (CH_3CN)_{0.33}(CH_2Cl_2)_{0.66}$	$C_{80}H_{80}Ag_4B_4F_{16}N_{12}O_8P_4$	$C_{40}H_{34}Ag_2F_6N_4O_8P_2 \cdot (C_4H_{10}O)_{0.5}$
fw	914.92	2240.16	1127.45
a (Å)	10.8716(9)	15.565(2)	9.343(1)
b (Å)	11.9998(9)	20.999(3)	31.912(5)
c (Å)	12.170(1)	28.131(4)	15.157(3)
α (deg)	94.502(5)		
β (deg)	100.834(5)		95.63(1)
γ (deg)	93.599(4)		
V (Å^3)	1549.7(2)	9195(2)	4497(1)
Z	2	4	4
space group	P-1	$P2_12_12_1$	$P2_1/n$
T (K)	110	110	110
D_{calcd}(g cm^{-3})	1.961	1.618	1.665
μ (mm^{-1})	1.671	1.000	1.024
$2\theta_{max}$, deg	62.40	46.52	52.00
reflns measured	20219	67540	38630
reflns used (R_{int})	9442 (0.0400)	13167(0.0836)	8838(0.0809)
restraints/params	56/431	0/1147	6/601
R1, [$I > 2\sigma(I)$]	0.0459	0.0464	0.0497
wR^2, [$I > 2\sigma(I)$]	0.1136	0.1126	0.1073
$R(F_o^2)$ (all data)	0.0755	0.0543	0.0797
$R_w(F_o^2)$ (all data)	0.1281	0.1177	0.1204
GOF on F^2	1.016	1.112	1.027

in 15 mL of toluene was then added over 15 min. The solution was stirred for 1 h and then allowed to warm to room temperature. The resultant, thick cloudy mixture was reduced to three-fourths of its original volume under vacuum and immediately filtered through Celite and washed with 5 mL of cold toluene. The solvent was removed from the yellow solution in vacuo to leave the crude product as a pale yellow oil in 95% yield (2.12 g, 6.26 mmol). The oil was then extracted with 180 mL of hexanes to leave the final product, **1**, as a colorless oil in 77% yield (1.71 g, 5.28 mmol). ^{1}H NMR ($CDCl_3$, 298 K) δ: 4.87 (d,m, 4 H, J(PH) = 8.8 Hz), 7.34 (m, 2 H), 7.48 (m, 3 H), 7.681 (m, 4 H), 8.59 (m, 4 H). ^{31}P NMR ($CDCl_3$, 298 K) δ: 160.4 (sep, J(PH) = 7.3 Hz).

Synthesis of PCP-32AgOTf (2). To a stirred solution of AgOTf (0.158 g, 0.615 mmol) in 3 mL of CH_3CN was added **1** (0.100 g, 0.308 mmol) in 3 mL of CH_3CN. The resulting solution was allowed to stir for 3 min and then dried in vacuo to leave a fluffy, off-white solid. The solid was then repeatedly redissolved in a small amount of CH_3CN and precipitated with ether until compound **2** was obtained as a white powder in 86% (0.22 g, 0.26 mmol) yield upon drying. Colorless plates of **2** were obtained by slow diffusion of ether into a solution of **2** in CH_2Cl_2 at 5 °C. ^{1}H NMR (CD_3CN, 298 K) δ: 5.11 (d,m, 4H), 7.47 (m, 2H), 7.65 (m, 3H), 7.85 (m, 4H), 8.12 (m, 4H). ^{31}P NMR (238 K) δ: 146.4 (d, J(Ag−P) = 908.2 Hz). Anal. Calcd for $C_{23}H_{20.5}N_{2.5}O_{8.5}PS_2F_6Ag_2$: C, 30.94; H, 2.31; N, 3.92. Found: C, 30.66; H, 2.37; N, 3.61.

Synthesis of PCP-32AgBF$_4$ (3). To a stirred solution of $AgBF_4$ (0.120 g, 0.616 mmol) in 3 mL of CH_3CN was added **1** (0.198 g, 0.610 mmol) in 3 mL of CH_3CN. The resulting solution was allowed to stir for 2 min and then dried in vacuo to leave an off-white powder. This was then dissolved in a small amount of CH_3CN and precipitated with ether, repeating until compound **3** was obtained as a white powder upon drying in 93% (0.29 g, 0.57 mmol) yield. Colorless plates of **3** were obtained by slow diffusion of ether into a solution of **3** in CH_3CN at 5 °C. ^{1}H NMR (CD_3CN, 298 K) δ: 5.07 (d,m, 4H), 7.45 (m, 2H), 7.65 (m, 3H), 7.85 (m, 4H), 8.48 (d, 2H), 8.55 (s, 2H). ^{31}P NMR (238 K) δ: 149.8 (d, J(Ag−P) = 804.7 Hz). Anal. Calcd for $C_{18}H_{17}N_2O_2PAgBF_4$: C, 41.66; H, 3.30; N, 5.40. Found: C, 41.15; H, 3.27; N, 5.30.

Synthesis of PCP-32Ag(tfa) (4). To a stirred suspension of Ag(tfa) (0.136 g, 0.615 mmol) in 5 mL of CH_2Cl_2 was added **1** (0.100 g, 0.308 mmol) in 5 mL of CH_2Cl_2. This was allowed to stir for 5 min until the solid Ag(tfa) was dissolved, after which time a brown oil precipitated. The solution was dried in vacuo to leave a fluffy brown powder. This was then dissolved in a small amount of CH_3CN and precipitated with ether. This was repeated until the off-white powder, **4**, was obtained in 94% (0.22 g, 0.29 mmol) yield. Colorless blocks of **4** were obtained by the vapor diffusion of ether into a solution of **4** in CH_3CN at 5 °C. ^{1}H NMR (CD_3CN, 298 K) δ: 5.12 (d,m, 4H), 7.39 (m, 2H), 7.59 (m, 3H), 7.82 (m, 4H), 8.50 (d, 2H), 8.59 (s 2H). ^{31}P NMR (238 K) δ: 152.2. Anal. Calcd for $C_{23.5}H_{18.75}N_{2.25}O_{6.25}PAg_2F_6$: C, 35.58; H, 2.38; N, 3.97. Found: C, 35.86; H, 2.40; N, 3.78.

X-ray Crystallographic Analysis. Crystallographic data were collected on crystals with dimensions 0.081 × 0.097 × 0.196 mm for **2**, 0.168 × 0.140 × 0.041 mm for **3**, and 0.070 × 0.090 × 0.100 mm for **4**. Data were collected at 110 K on a Bruker X8 Apex using Mo Kα radiation (λ =0.710 73 Å). All structures were solved by direct methods after correction of the data using SADABS.[49] Crystal data are presented in Table 1, and selected interatomic distances and angles and other important distances are given in Table 2. All of the data were processed using the Bruker AXS SHELXTL software, version 6.10.[50] Unless otherwise noted, all non-hydrogen atoms were refined anisotropically and hydrogen atoms were placed in calculated positions. The crystal structure of **2** contains a disordered solvent position that is occupied in part by a molecule of dichloromethane and in part by a molecule of acetonitrile. The crystal structure of **3** contains four solvent molecules of acetonitrile and four noncoordinating BF_4^- anions, two of which are disordered over two positions. Compound **4**'s crystal structure contains an ether solvent molecule whose disorder is linked to the disorder of the C32 phenyl ring.

Results and Discussion

Synthesis and NMR Spectroscopy. Compound **1** is made by a procedure similar to that reported for the synthesis of

(49) Sheldrick, G. M. *SADABS*; University of Gottingen: Gottingen, Germany, 1997.
(50) Sheldrick, G. M. *SHELXTL*, version 6.10; Bruker AXS, Inc.: Madison, WI, 2000.

Table 2. Selected Bond Lengths (Å) and Angles (deg) and Important Distances for 2−4

2, **PCP-32AgOTf**			
Ag1−O6	2.287(3)	Ag1−P1	2.323(1)
Ag1−O3#1	2.434(3)	Ag1−O3	2.456(3)
Ag2−N2	2.152(4)	Ag2−N1	2.156(3)
Ag2−Ag2#2	3.1918(8)	P1−N1	5.161(3)
P1−N2#2	5.487(4)	N1−N2#2	3.466(5)
Ag1−Ag1#1	3.8137(7)	Ag1−Ag2	6.5088(7)
Ag1−Ag2#2	6.7435(7)	O6−Ag1−P1	144.84(7)
O6−Ag1−O3#1	84.0(1)	P1−Ag1−O3#1	122.30(7)
O6−Ag1−O3	82.6(1)	P1−Ag1−O3	122.99(7)
O3#1−Ag1−O3	77.5(1)	N2−Ag2−N1	172.3(1)
N2−Ag2−Ag2#2	112.5(1)	N1−Ag2−Ag2#2	75.2(1)
3, **PCP-32AgBF$_4$**			
Ag1−N1	2.289(6)	Ag1−N2	2.296(6)
Ag1−P1	2.3363(19)	Ag2−N3	2.274(6)
Ag2−N4	2.318(7)	Ag2−P2	2.348(2)
Ag3−N5	2.265(6)	Ag3−N6	2.285(6)
Ag3−P3	2.362(2)	Ag4−N7	2.268(6)
Ag4−N8	2.295(6)	Ag4−P4	2.352(2)
P1−N3	6.195(6)	P1−N8#4	5.906(7)
N3−N8#4	8.743(8)	P2−N5	6.165(7)
P2−N2#1	5.860(7)	N5−N2#1	8.541(9)
P3−N7	6.145(6)	P3−N4#11	5.999(7)
N7−N4#11	8.444(9)	P4−N1#6	6.061(6)
P4−N6#3	5.956(7)	N1#6−N6#3	8.769(9)
Ag1−Ag2	9.287(1)	Ag1−Ag4#5	9.024(1)
Ag2−Ag4#5	8.648(1)	Ag2−Ag3	9.454(1)
Ag2−Ag1#1	9.099(1)	Ag3−Ag1#1	8.763(1)
Ag3−Ag4	9.597(1)	Ag3−Ag2#2	9.324(1)
Ag4−Ag2#2	8.648(1)	Ag4−Ag1#6	9.263(1)
Ag4−Ag3#4	9.208(1)	Ag1#7−Ag3#4	8.763(1)
Ag1−F16#8	2.90(1)	Ag2−F7#9	2.92(1)
Ag3−F8#10	2.87(2)	Ag4−F15#11	2.73(1)
N(1)−Ag(1)−N(2)	93.1(2)	N(1)−Ag(1)−P(1)	132.4(2)
N(2)−Ag(1)−P(1)	133.1(2)	N(3)−Ag(2)−N(4)	99.4(2)
N(3)−Ag(2)−P(2)	134.4(2)	N(4)−Ag(2)−P(2)	125.6(2)
N(5)−Ag(3)−N(6)	107.3(2)	N(5)−Ag(3)−P(3)	127.8(2)
N(6)−Ag(3)−P(3)	124.1(2)	N(7)−Ag(4)−N(8)	98.3(2)
N(7)−Ag(4)−P(4)	136.4(2)	N(8)−Ag(4)−P(4)	124.4(1)
4, PCP-32Ag(tfa)			
Ag1−N2#1	2.297(4)	Ag1−P1	2.357(1)
Ag1−O3	2.386(4)	Ag1−O3#2	2.509(4)
Ag2−N3#3	2.322(4)	Ag2−P2	2.329(1)
Ag2−O7	2.344(4)	Ag2−N1	2.355(4)
P1−N1	6.203(4)	P1−N2	5.520(5)
P2−N3	6.108(4)	P2−N4	5.651(5)
N1−N2	10.774(6)	N3−N4	10.026(6)
Ag1−Ag2	9.112(1)	Ag1−Ag1#1	6.466(1)
Ag1#1−Ag2	14.015(2)	Ag2−Ag2#3	9.227(1)
N(2)#1−Ag(1)−P(1)	132.5(1)	N(2)#1−Ag(1)−O(3)	94.1(1)
P(1)−Ag(1)−O(3)	126.8(1)	N(2)#1−Ag(1)−O(3)#2	87.9(1)
P(1)−Ag(1)−O(3)#2	122.5(1)	O(3)−Ag(1)−O(3)#2	74.4(1)
N(3)#3−Ag(2)−P(2)	125.4(1)	N(3)#3−Ag(2)−O(7)	86.8(1)
P(2)−Ag(2)−O(7)	133.3(1)	N(3)#3−Ag(2)−N(1)	98.2(1)
P(2)−Ag(2)−N(1)	116.3(1)	O(7)−Ag(2)−N(1)	86.4(1)

[a] Symmetry transformations used to generate equivalent atoms: For **2**: #1 = $-x+1, -y, -z+2$; #2 = $-x+1, -y, -z+1$. For **3**: #1 = $-x+1, y+1/2, -z+1/2$; #2 = $-x, y+1/2, -z+1/2$; #3 = $-x+1, y-1/2, -z+1/2$; #4 = $-x-1, y+1/2, -z+1/2$; #5 = $-x, y-1/2, -z+1/2$; #6 = $-x-1, y-1/2, -z+1/2$; #8 = $x-2, y-1, z$; #9 = $x-0.5, -y+0.5, -z+1$; #10 = $x-1, y, z-1$; #11 = $-x, y-0.5, -z+0.5$. For **4**: #1 = $-x+1, -y+1, -z+1$; #2 = $-x+2, -y+1, -z+1$; #3 = $x-1/2, -y+3/2, z-1/2$.

the singly substituted derivative, diphenylphosphino-3-pyridylcarbinol, adjusting for the addition of a second equivalent of carbinol to the phosphine. **PCP-32** is seen to be quite a bit more sensitive to reaction conditions than its singly substituted counterpart and decomposes at a more rapid rate in solution at room temperature. After isolation as a colorless oil, **1** is found to be readily hydrolyzed, oxidizes in air, and decomposes with exposure to heat or light. The thermal instability is such that storage at a temperature of −35 °C is insufficient to halt the degradation of the fluid, colorless oil into a thick, dark-yellow cloudy oil over time. Pure **1** can be separated at any point, when necessary, from its decomposition products by extraction into hexanes. The ligand is, however, initially synthesized in sufficient purity to allow for further use without the final hexane extraction. ^{1}H and ^{31}P NMR spectra of **1** were obtained in $CDCl_3$ and show the pronounced three-bond coupling of phosphorus to the phenyl and methylene protons; a well-defined phosphorus septet is thus found centered at 159.9 ppm.

The silver compounds **2**−**4** were made by reaction of **1** with silver salts of the respective anions under ambient conditions and inert atmosphere. Solutions of the three compounds readily decompose to leave metallic silver and an unidentifiable black byproduct. However, the powders of each complex have proven themselves to be quite robust, withstanding long exposure to air and room temperatures with little sign of decomposition. They demonstrate a concomitant increase in photostability, showing only slight signs of decomposition for days upon exposure to light as opposed to hours for the analogous complexes of the monosubstituted $PPh_2(3\text{-}OCH_2C_5H_4N)$. This relative increase in solid-state stability could be accredited to the extra dimensionality that the second carbinol substitution imparts on the coordination of the ligand. Compounds **2**−**4** appear to be stable indefinitely in the solid state if stored in the dark and refrigerated under inert atmosphere. Variable-temperature ^{31}P NMR spectra were recorded to −35 °C in deuterated acetonitrile. At this temperature the dissociation of the Ag−P bond is slowed to a time scale where significant polymeric character is observed and the various Ag−P couplings can be readily seen.

Compound **2** is made by the mixing of 2 equiv of AgOTf with a solution of **1** in acetonitrile. A light brown color appears almost immediately upon mixing and is indicative of the reactions of **1** with the various silver salts. If left stirring at room temperature, this color rapidly grows more intense and eventually becomes cloudy, signifying decomposition of the coordination complex. Drying of the solution in vacuo yields a crude, oily brown powder that is purified with acetonitrile and ether. Upon drying of the precipitate **2** is collected as a white powder. Solutions of **2** in various solvents noticeably decompose within minutes at room temperature. However, when dichloromethane solutions layered with ether are kept at 5 °C, they are sufficiently stable to allow the growth of diffraction-quality crystals. Over time, oxidation of the ligand in solution results in precipitation of metallic silver. At room temperature a very broad phosphorus resonance is evident centered at 148.0 ppm in the ^{31}P spectrum, indicating at least some degree of Ag−P coupling in solution. Upon cooling to −35 °C this broad signal splits into a doublet of very sharp peaks centered slightly upfield at 146.4 ppm.

Scheme 2. Binding Modes of PCP-32 with Silver Salts

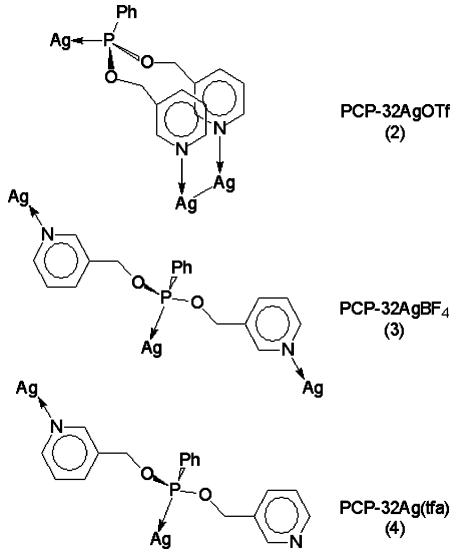

The coordination polymer, **3**, is obtained as an off-white powder by the reaction of $AgBF_4$ with a solution of 1 mol equiv of **1** in acetonitrile. Solutions of **3** also quickly develop a brown tint but do not undergo extensive decomposition in such a short time as for **2**. This increase in stability of the BF_4^- complex is analogous to the behavior of the $Ph_2P(3\text{-}OCH_2C_5H_4N)AgBF_4$ coordination polymer; the reasoning behind this has been previously theorized.[29] Tiny, colorless parallelepiped-shaped crystals of **3** were grown by slow diffusion of ether into a solution of **3** in acetonitrile at 5 °C. Room-temperature ^{31}P NMR spectra of **3** reveal a shouldered peak, due to Ph−H coupling, centered upfield from the free ligand at 149.0 ppm. The Ag−P coupling is not readily apparent in acetonitrile solution at 23 °C. Upon cooling to −35 °C a silver-split phosphorus doublet is again noticed, now centered at 149.8 ppm.

Complex **4** is seen to be highly prone to decomposition in solution, rapidly precipitating metallic silver and an oily black byproduct. To circumvent this difficulty the ligand was added to a suspension of Ag(tfa) in CH_2Cl_2, in which **4** is only sparingly soluble. In this manner, as the silver salt is drawn into solution by the forming coordination polymer it is immediately precipitated back out of solution, reducing the chance for decomposition. Reaction is apparent from the rapid replacement of the Ag(tfa) granules with a light-brown oily precipitate along with a slight darkening of the solution. Upon purification the compound is reclaimed as a finely divided colorless powder that quickly deposits metallic silver from solutions. Crystals of **4** were grown with some difficulty by vapor diffusion of ether into dilute solutions of **4** in acetonitrile at 5 °C. Solutions in high concentrations of **4** typically resulted in precipitation versus crystallization. ^{31}P NMR spectra of **4** show a single broadened phosphorus peak approximately 8 ppm upfield of the free ligand at 152.0 ppm. Lowering the NMR operating temperature to −35 °C shows a slight broadening (∼1 ppm) of the ^{31}P resonance, though the Ag−P coupling can still not be discerned.

X-ray Crystal Structures. The silver coordination environments as well as the twisted conformations of the carbinol portions of the ligand in each of the structures are quite diverse. Silver geometries range from the near linear 172.3(1)° of Ag2 in **2** to the distorted tetrahedrons of the silvers in **4**. Scheme 2 gives a representation of the different binding modes displayed by **PCP-32**. The two carbinol substitutions of each ligand are, as expected, capable of a variety of rotations and extensions allowing the py−Ag binding of the two "arms", in relation to one another, to go from nearly parallel and co-directional in **2** to pointing in nearly opposite directions in **3**. The flexibility of the $-OCH_2-$ spacer groups also allow for a broad range of metal−metal distances to be had by the N-bound silvers of the ligand. This interval spans from the very close Ag−Ag interaction of **2** at 3.1918(8) Å to the outstretching reach of 14.015(2) Å in **4**. With the 1:2 ratio of P to N in the ligand, a strict head-to-tail-type coordination throughout the polymer analogous to those seen in the **PCP-31** structures is difficult to achieve and is therefore not observed in any of the structures. There is instead a mixture of Ag coordination environments within **2** and **4** and a repetitive head-to-tail-to-tail motif apparent in **3**. All of these structural arrangements are spawned from the varying degrees of interaction that are seen by the different anions. With both of the structures containing oxygen donor anions, at least partial oxide bridging is apparent between some of the silver atoms. Conversely, in the case of BF_4^- there is no anionic bridge and only a slight M−anion interaction that merely serves to hold the BF_4^- in position in the lattice.

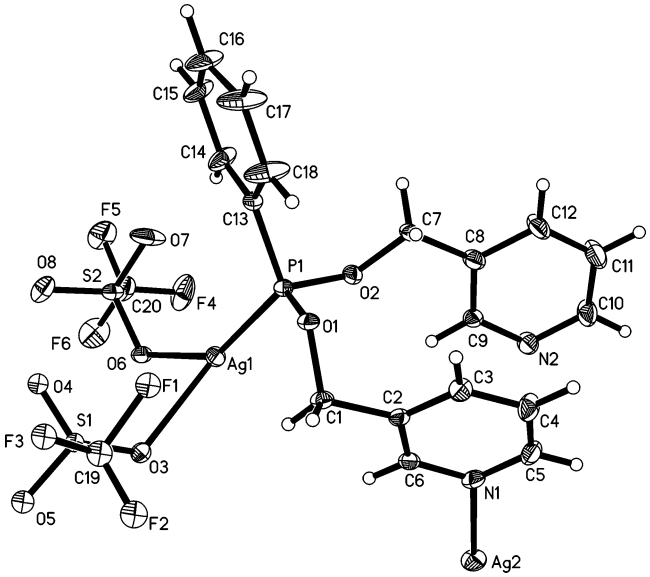

Figure 1. Thermal ellipsoid plot of the unique portion of the **PCP-32AgOTf** polymer. Ellipsoids are drawn at the 30% probability level.

The molecular structure of compound **2** contains two distinct silver environments representative of the coordination extremes shown herein. Both a pseudo-two-coordinate and a four-coordinate arrangement are displayed. A thermal ellipsoid plot of the unique portion of this structure is shown in Figure 1. The two unique metal centers are repeated in one dimension, linked by bridging anions, to form the linear coordination polymer as demonstrated in Figure 2. Ag1 is bridged via one oxygen atom of each of two separate triflates

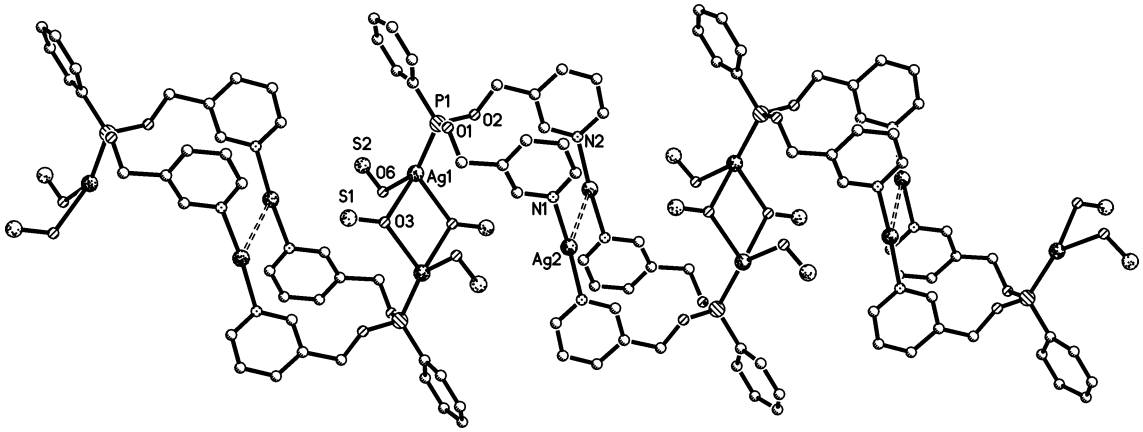

Figure 2. View of the 1-D chain of **PCP-32AgOTf**, **2**. H atoms and the noncoordinating portion of the triflates have been removed for clarity.

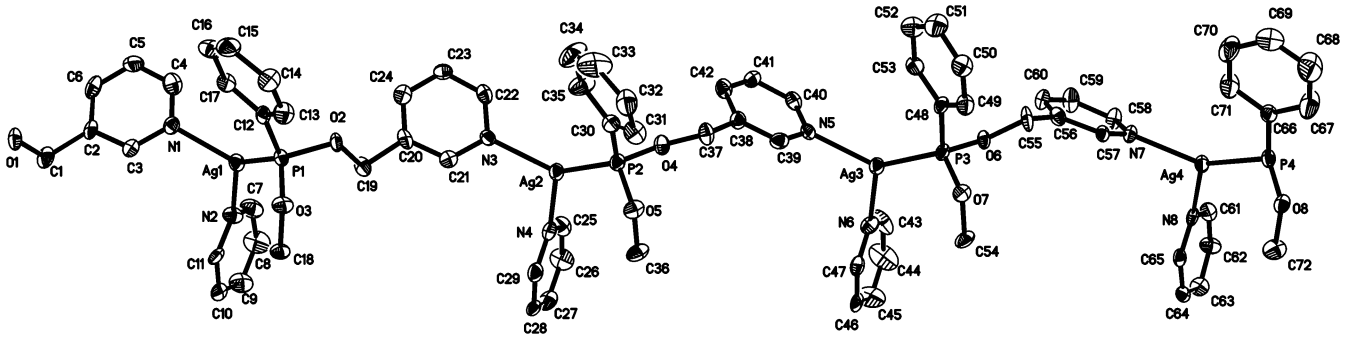

Figure 3. Thermal ellipsoid plot of the cationic unique portion of the **PCP-32AgBF$_4$** polymer. The partial spiral of the pyridyl linkages through the linear chain is apparent. Ellipsoids are drawn at the 50% probability level. H atoms have been removed for clarity.

to an opposing, symmetry-equivalent P-bound Ag. The tetrahedron of P and O around Ag1 is completed by a terminal triflate bound to each metal. This effectively imposes a −2 charge on the Ag_2OTf_4 cluster that balances the positive charge levied across the ligand at the N-bound silvers. It is seen that the coordinating triflates are only observed at the phosphorus-bound Ag centers. This enforces a very prominent trans-ligand static charge separation. The two pyridyl rings of each ligand are brought within close proximity of one another at 3.466(5) Å, possibly by slight $\pi-\pi$ interactions of the adjacent aromatic rings. The planes of these rings are seen to be nearly parallel though the N2 pyridyl is disordered over two positions as it hinges about the N−Ag bond. This close positioning of pyridyl donors allows for the N-bound silvers to come within 3.1918(8) Å of each other, leading to a respectable Ag−Ag interaction that likely has an influence on the luminescence of this species. The average cross-ligand distance observed separating the P- and N-bound silvers is 6.626 Å, from which is given some indication of the amount of charge separation present. Intraligand P−N distances vary slightly from P1−N1 to P1−N2A at 5.161(3) and 5.487(4) Å, respectively. The Ag−P bonds display typical values at 2.323(1) Å, while the N−Ag bonds are noticeably short with an average of 2.155 Å. This is undoubtedly due to the charge density present on the N-bound silvers that is not balanced by a closely associated anion. Ag(1)−O distances vary from 2.287(3) to 2.456(3) Å with the shorter value represented by the terminal bound triflate. Ag1 is in a severely distorted tetrahedral arrangement with its oxygen-only face being constricted by the bridging trifluoroacetates and displaying O−Ag−O angles from 77.5(1)° to 84.0(1)°. The O−Ag−P angles are in turn widened from 122.30(7)° to 144.84(7)°. The environment of Ag2 is nearly linear with respect to pyridyl coordination with an N−Ag−N angle of 172.2(1)°. This slight distortion results from the movement of the Ag toward its symmetry equivalent, which is slightly askew from Ag2. The N−Ag−Ag angles, at 75.2(1)° and 112.5(1)°, show one silver to be oriented slightly above the other.

A thermal ellipsoid plot of the unique portion of **3** is shown in Figure 3. In the structure of **3** we see four crystallographically inequivalent silver centers arranged linearly whose differences arise from a slight twisting of the ligands through the length of the unique portion. However, rather than a fully spiraling polymer, only a partial helix is seen to repeat throughout the lattice. This partial spiral is evident in either of the two dimensions in which the polymer is perpetuated and is demonstrated in Figure 4. This two-dimensional growth of **3** gives rise to an infinite pleated sheet structure with anions dispersed throughout the crevices of the layers. A view of how these 2-D layers pack together is shown in Figure 5. Opposing the trend of structures **2** and **4**, all silvers in **3** are identical in connectivity, being coordinated by two pyridyls and one phosphorus donor in a doubly distorted trigonal arrangement. The first distortion involves the angles which for the N−Ag−N junction are all acute from 93.1(2)° to 107.3(2)°, while the other two N−Ag−P angles are widened to values of 124.1(2)° to 136.4(2)°. The second distortion stems from the long-distance interaction of a BF_4^- fluorine approaching at an average proximity of 2.8 Å to

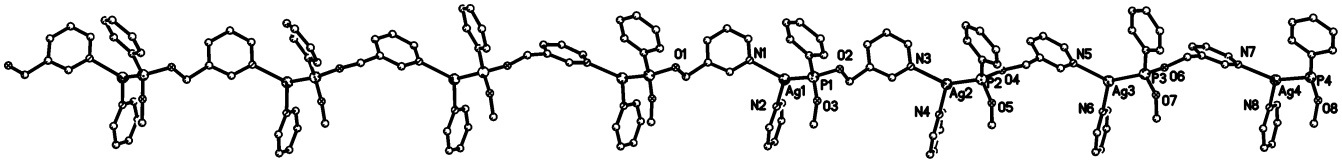

Figure 4. View of the chain of **PCP-32AgBF$_4$**, **3**, perpetuated in one dimension. The partial spiral of the pyridyl linkages can be seen to abruptly restart at the end of the unique portion. H atoms have been removed for clarity.

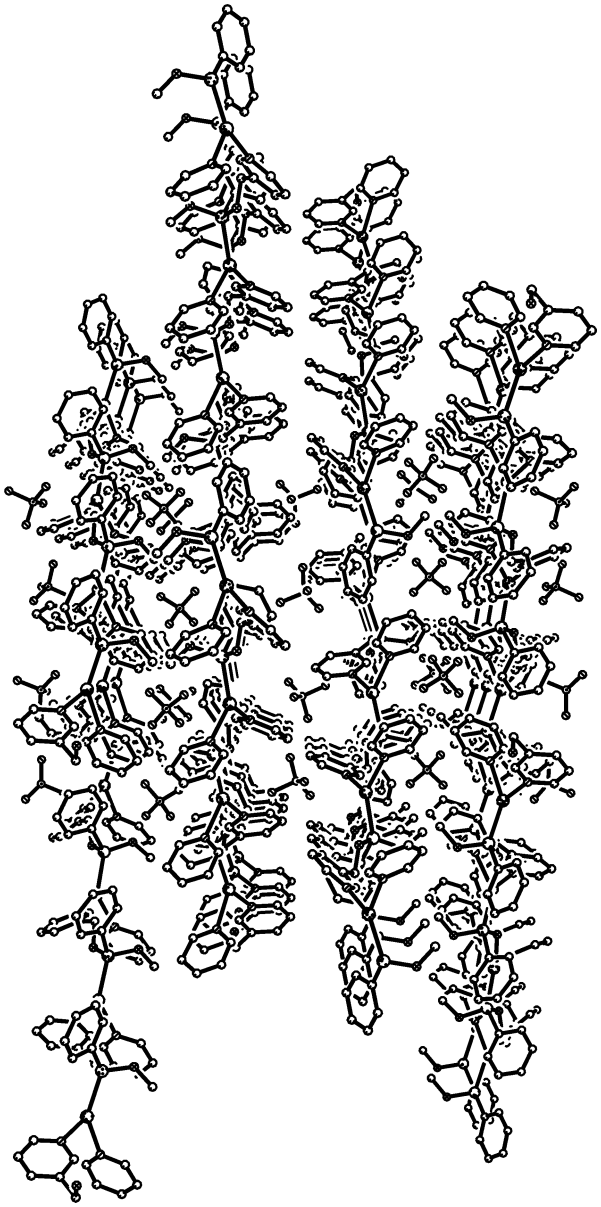

Figure 5. View down the *a* axis of how the 2-D sheets of **PCP-32AgBF$_4$** stack together encompassing the BF_4^- anions. H atoms have been removed for clarity.

the metal. As the metal centers are pulled out of their N−N−P coordination planes, a resulting mean perturbance of 0.121 Å is seen. All Ag−N and Ag−P bonds show typical lengths with ranges of 2.265(6)−2.318(7) and 2.336(2)−2.362(2) Å, respectively. Overall, intraligand P−N distances show an increase in length of close to 1 Å from **2**. Averages are 5.932 Å on the outstretched pyridyl arms and 6.142 Å on the collinear pyridyls. This results in an increase in separation of P- and N-bound silvers; the magnitude of this separation depends upon the orientation of the pyridyl extension. Those silvers contained within the collinear backbone of the structure have separations from 9.263(1) to 9.597(1) Å, while those arranged nearly perpendicular have slightly smaller values from 9.024(1) to 9.324(1) Å. This accompanies a substantial increase in cross-ligand metal−metal separation of the N-bound silvers, whose distance in **3** averages at 8.7055 Å. **3** crystallizes in the noncentrosymmetric space group $P2_12_12_1$ with a refined Flack parameter of 0.00(2).

Compound **4** forms a structurally complicated polymer that displays a variety of interesting attributes. Figure 6 shows the molecular structure of the unique portion of **4**. This winding 3-D growth is displayed in Figure 7. Growth of the polymer occurs in three dimensions due to the bridging actions of both the ligand and the trifluoroacetates. The ligand in this case occupies two separate roles within the structure. In the first instance the phosphonite is tridentate using all three binding sites to coordinate to two different types of metal centers. Using one pyridyl "arm" and the phosphorus, two equivalent silvers, Ag1 and Ag1#1, are bound by two symmetry-equivalent ligands in a head-to-tail fashion forming a ring. Each of these silvers is subsequently bridged by two η^1,μ_2−trifluoroacetates to yet another equivalent metal. The remaining "arm" of the ligand extends from the ring and acts as a bridge to the other unique silver of the polymer, Ag2. It is as a result of this outstretching reach that we see the greatest cross ligand metal−metal distance of the three polymers. The N-bound silvers of these oppositely directed donors are separated by a distance of 14.015(2) Å across the breadth of the ligand. The P-bound to N-bound metal distances across this ligand show separations of 9.112(1) and 6.466(1) Å for Ag1−Ag2 and Ag1−Ag1A, respectively. Ag2 is bound by the phosphorus and nitrogen of two separate but equivalent ligands that are in a similar conformation to that of the one P-bound to Ag1 and the pyridyl that bridges to Ag1 to achieve a head-to-tail-to-tail motif. In this case, however, the ligands are not involved in ring formation. The attached ligands instead continue off via one pyridyl extension each in two separate polymeric strands that run parallel to one another. The remaining "arm" of this ligand is a curious feature in that it has a noncoordinating "dangling" pyridyl that sits within the space between ligands. It is believed that the steric packing that encapsulates this particular pyridyl ring is responsible for its unsaturated coordination state since even when an excess of Ag(tfa) is used the noncoordinating nitrogen is present in the crystal structure. The similar conformations of the two unique ligands in the structure of **4** likewise display similar intraligand N−N distances at 10.774(6) Å for the P1 ligand and 10.026(6) Å for that of P2. Comparable P−N distances

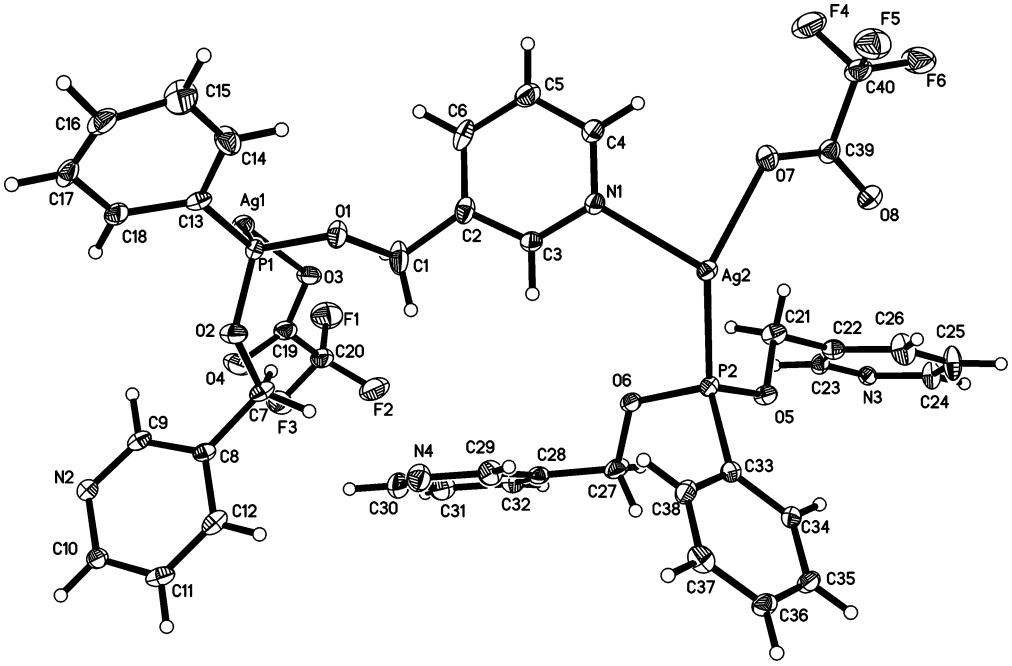

Figure 6. Thermal ellipsoid plot of the unique portion of **PCP-32Ag(tfa)**, **4**. Ellipsoids are drawn at the 30% probability level. As shown, N4 is seen to be noncoordinating. All other pyridyl donors are metal bound.

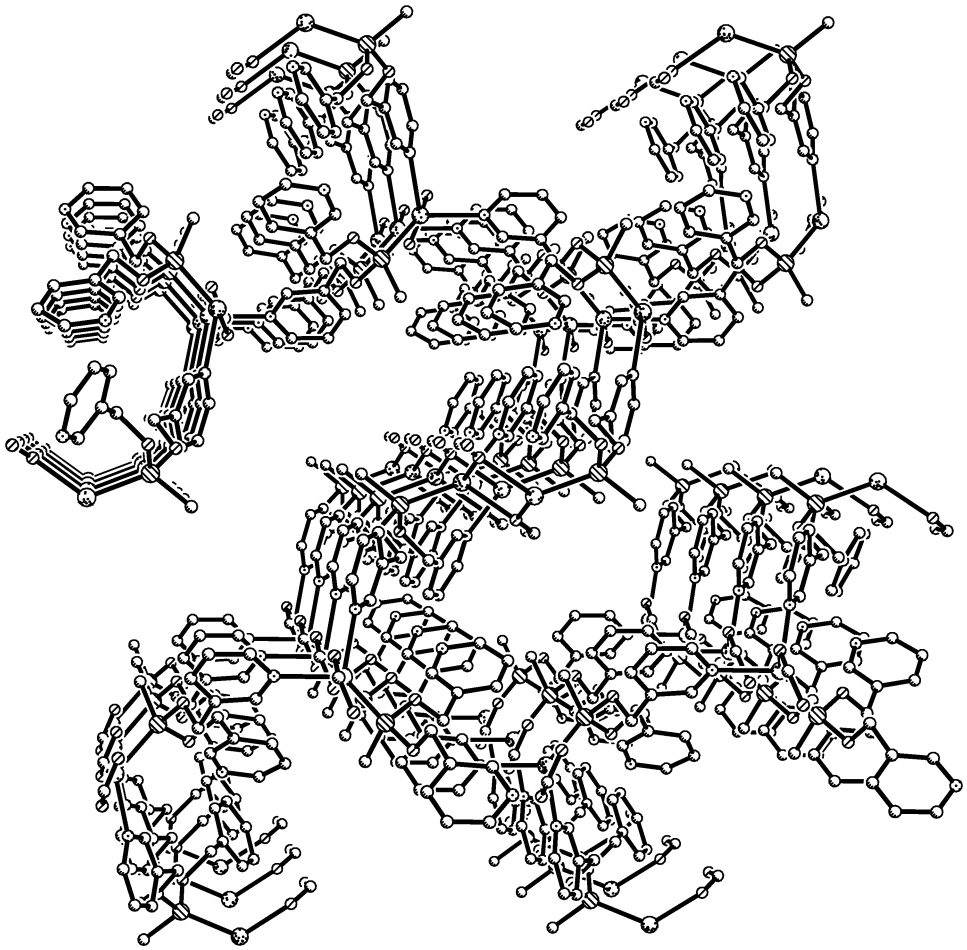

Figure 7. Packing structure of complex **4** showing the 3-D growth of the polymer. H atoms, trifluoromethyls, and all but the *ipso* portion of the phenyl rings have been removed for clarity.

are also noticed with each ligand having a short and long stretch: P1−N2 and P1−N1 separations are 5.520(5) and 6.203(4) Å, respectively, while the analogous P2−N4 and P2−N3 distances are 5.651(5) and 6.108(4) Å. The single cross-ligand metal−metal distance of the P2 ligand is that of the P2 to N3 silvers, which is slightly longer than that of

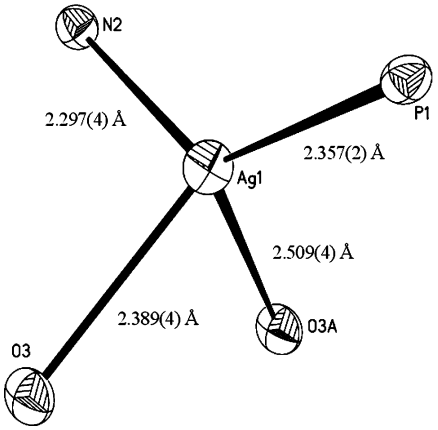

Figure 8. Coordination environment of Ag1 in the polymer of **4**. Ellipsoids are drawn at the 50% probability level.

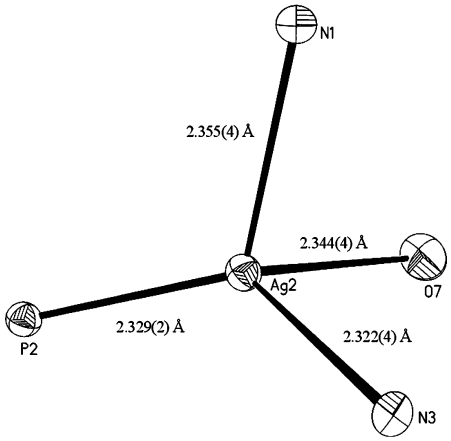

Figure 9. Coordination environment of Ag2 in the polymer of **4**. Ellipsoids are drawn at the 50% probability level.

the P1 ligand at 9.227(1) Å. Both silver centers here are in distorted tetrahedral arrangements. The coordination around Ag1 is completed by one pyridyl and phosphorus donor as well two bridging trifluoroacetate oxygens and is shown in a close-up view in Figure 8. The Ag1−N2#1 bond is only slightly stretched for a Ag−pyridyl distance at 2.297(4) Å, while the Ag1−P1 bond is a typical 2.357(2) Å. Bonds to the bridging trifluoroacetates are seen to be inequivalent with Ag1−O3 at 2.386(4) Å and Ag1−O3#2 at 2.509(4) Å. It is also noticed that the small bridging distance of the η^1,μ_2-trifluoroacetates constrict the angle they create with the metal to an acute 74.4(1)°. As a result, the P1−Ag1−N1 angle has room to spread apart, which is apparent with a 132.5-(1)° angle. The remaining angles around Ag1 are also distorted from the ideal tetrahedral geometry and have values interspersed between the aforementioned extremes. In the absence of the bridging trifluoroacetates displayed by Ag1, the distortions of the tetrahedral coordination sphere of Ag2 are not seen to be as severe. The environment of Ag2 is displayed in Figure 9 and includes two pyridyl donors, the phosphorus atom P2, and a terminal bound η^1-trifluoroacetate. The silver−pyridyl linkages in this case are uncommonly lengthy at 2.355(4) and 2.322(4) Å for Ag2−N1 and Ag2−N3#3, while the Ag2−P2 and Ag2−O7 bonds are in the typical range at 2.329(1) and 2.344(4) Å, respectively. The angles about Ag2 however are still shown to be rather extreme from 86.4(1)° to 133.3(1)°.

Luminescent Properties. Mixed inorganic−organic coordination polymers have been recently explored as having potential as new "organic" light-emitting devices, OLEDs. The advantage of these hybrids over the strictly organic luminescent materials is the ability to tune their absorption and emission by altering the metal environment. This variability stems from either metal-to-ligand or ligand-to-metal charge transfer, which is obviously not an option with the traditional organic LED.[51] All excitation and emission spectra were recorded at concentrations of 1×10^{-4} M in acetonitrile glasses at 77 K. These spectra are demonstrated in Figure 10. The resemblance of the excitation spectra of compounds **2**−**4** with that of the free $PhP(3\text{-}OCH_2C_5H_4N)_2$ ligand are suggestive of a ligand-based absorption which then decays by means of ligand-to-metal charge transfer. The excitation spectrum of the free ligand **1** shows two maxima at 298 and 352 nm. Excitation maxima for **2**, **3**, and **4** are 295, 297, and 305 nm, respectively. Emission spectra for all compounds **1**−**4** show multiple maxima, illustrating the complexity of the decay transitions associated with such a complicated system. The ligand itself demonstrates several emission maxima across a wide section of the spectrum. Peaks are seen at 412, 442, 474, and 544 nm. A great deal of free ligand character is seen in the spectrum of **3**, which is the weakest emitter of the silver complexes. Peaks are seen at 412, 441, and 477, and a shoulder is noticed at ∼547 nm. This suggests that the emission is mainly a ligand-based one intensified by metal coordination. The emission of the silver triflate complex is much more intense and covers a broader spectral range than either **1** or **3**. Peaks are displayed at 363, 404, 423, 438, 452, and 501 nm, and again a shoulder

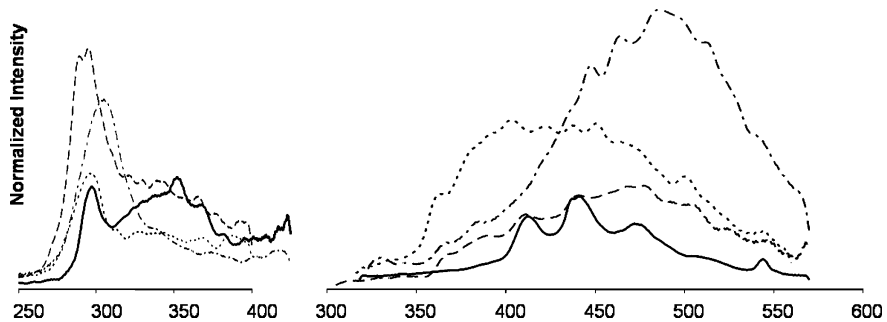

Figure 10. Normalized excitation and emission spectra of compounds **1**−**4** taken in acetonitrile glasses at 1×10^{-4} M at 77 K: (—) PCP-32, (- - -) PCP-32AgBF$_4$, (· · ·) PCP-32AgOTf, (- · -) PCP-32Ag(tfa).

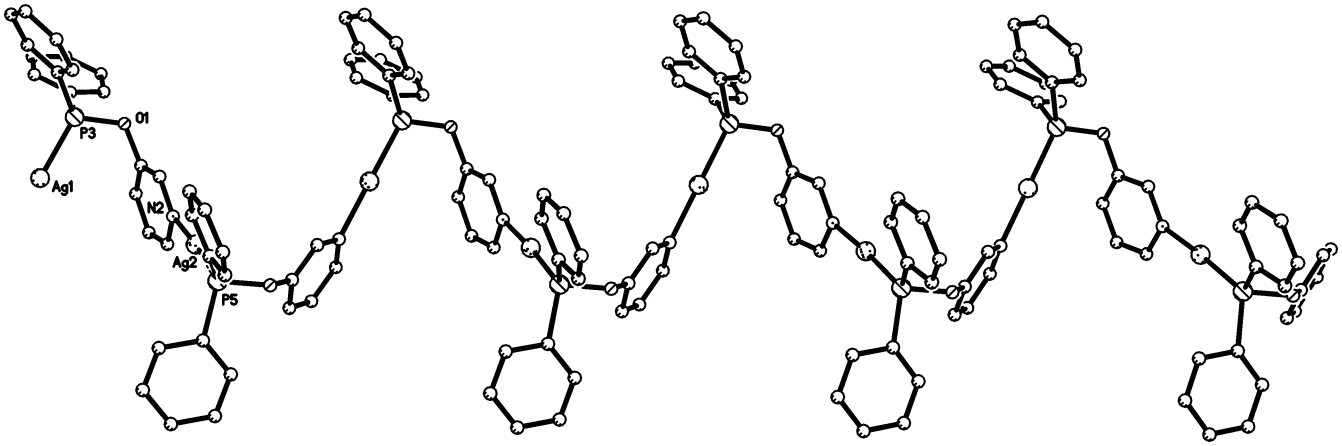

Figure 11. View of the cationic polymer formed in the reaction of **PHP-31** with $AgPF_6$. H atoms have been removed for clarity.

is noticed at 547 nm. The emission spectrum of complex **4** is noticeably more intense than the others, as expected from visual observations, and is also slightly red shifted. The local maxima for this complex are seen at 449, 465, 487, and 513 nm.

Conclusions

We demonstrated in this study the versatility of the phosphonite $PhP(3\text{-}OCH_2C_5H_4N)_2$ in the formation of anion-dependent, luminescent coordination polymers. The flexibility of the pyridyl extensions allowed trans-ligand metal−metal distances to span a range of over 10 Å from 3.1918(8) to 14.015(2) Å. These pyridyl arms were seen to adopt conformations ranging from parallel to opposed. The silver coordination environment, dimensionality of the polymers, and luminescence characteristics are all seen to be dependent upon the anion present. We are currently exploring the coordination and luminescence properties of silver complexes of the trisubstituted analogue of the phosphonite as well as their closely related 2- and 4-pyridyl-substituted isomers. We are also studying the coordination properties of these ligands with other metals that have more of a preference for phosphorus versus nitrogen, or vice versa, in their coordination. It is also of interest to determine what changes in activity are noticed by altering the rigidity of these ligands by addition or subtraction of atoms between the phosphorus and pyridyl rings. Preliminary structural studies of the silver(I) coordination complexes formed by the **PHP-31** ligand (the hydroxypyridine-derived analogue of **PCP-31**) show polymers much like those of the **PCP** ligands but are obviously more restricted in their arrangements. An example of this is shown in Figure 11, where the complex **PHP-31AgPF$_6$** demonstrates its cationic 1-D polymer of two-coordinate silver.

Acknowledgment. This research was supported by funds provided by the University Research Committee at Baylor University (019-F00-URC and 011-N02-URC), a grant provided by the Vice-Provost for Research at Baylor University, and a grant from the Robert A. Welch Foundation (AA-1508). The Bruker X8 APEX diffractometer was purchased with funds received from the National Science Foundation Major Research Instrumentation Program, Grant CHE-0321214.

Supporting Information Available: Extra figures as well as a listing of the final atomic coordinates, anisotropic thermal parameters, and complete bond lengths and angles in CIF format are available for complexes **2**−**4**. This material is available free of charge via the Internet at http://pubs.acs.org.

IC0486365

(51) Bacher, A.; Erdelen, C. H.; Paulus, W.; Ringsdorf, H.; Schmidt, H.-W.; Schuhmacher, P. *Macromolecules* **1999**, *32*, 4551−4557.